



ORIGINAL ARTICLE

Antibacterial susceptibility of new copper(II) N-pyruvoyl anthranilate complexes against marine bacterial strains – In search of new antibiofouling candidate



Reda F.M. Elshaarawy ^{a,*}, Christoph Janiak ^b

^a Chemistry department, Faculty of Science, Suez University, Suez, Egypt

^b Institut für Anorganische Chemie und Strukturchemie, Heinrich-Heine Universität Düsseldorf, 40204 Düsseldorf, Germany

Received 25 February 2015; accepted 12 April 2015

Available online 18 April 2015

KEYWORDS

Chemoselective aminolysis;
Thenoyl-pyruvanthranilic;
Cu(II)-complexes;
Bactericidal;
Antibiofouling

Abstract Biofouling is a serious problem and very difficult to overcome, since the marine biofilm-producing microorganisms resist the host defense mechanism and antibiotic therapy. Therefore, there is an urgent need to develop potent anti-biofouling agent to effectively eradicate unwanted biofilms. Our work represents antibacterial susceptibility and antibiofilm forming assay of new copper(II) N-pyruvoyl anthranilate architectures (**4a–d**) against *Staphylococcus aureus* and *Escherichia coli*, marine isolates. The preliminary biofilm susceptibility tests revealed that, the most potent staphylococcalcidal (MIC/MBC = 9.25/10.50 mM) and *E. coli*-cidal (MIC/MBC = 13.25/13.50 mM) agent, **4d**, exhibits significant biofilm inhibition. Complex **4d** can therefore provide an antibiofilm-forming agent candidate to curb the formation of biofilms.

© 2015 The Authors. Production and hosting by Elsevier B.V. on behalf of King Saud University. This is an open access article under the CC BY-NC-ND license (<http://creativecommons.org/licenses/by-nc-nd/4.0/>).

1. Introduction

Interestingly, α -Keto amides formed from reaction of (Het)aroylpyruvic acid esters with amines, to form

* Corresponding author. Tel.: +20 1017377216.

E-mail addresses: reda_elshaarawi@science.suez.edu.eg, Reda.El-Shaarawy@uni-duesseldorf.de (R.F.M. Elshaarawy), janiak@uni-duesseldorf.de (C. Janiak).

Peer review under responsibility of King Saud University.



Production and hosting by Elsevier

aroylpyruvic acid amides, offer various drug-design opportunities and important suitable alternative approaches for the delivery of biologically active compounds, for examples in anti-inflammatory (Kožmynikh et al., 1992), antibacterial (Milyutin et al., 1997; Yanborisov et al., 1989), analgesic and antispasmodic, chemotherapy with extraordinarily low toxicity (Kožmynikh et al., 2002). Furthermore, oxanilic acids have been reported as inhibitors of protein-tyrosine phosphatase 1B (PTP1B) (Andersen et al., 2002; Iversen et al., 2001), T-cell protein-tyrosine phosphatase (Iversen et al., 2002) and the tyrosine kinase p56^{lck} SH2 domain (Beaulieu et al., 1999). Oxanilic acid esters have been found to be potent orally active antiallergy agents (Sellstedt et al., 1975; Wright and Johnson, 1977; Klaubert et al., 1981; Hargrave et al., 1983).

It has also been reported (Matsoukas et al., 1988) that, substitution of the sarcosine residue of sarmesin with oxanilic acid yields analogues (Scheme S1, supplementary information) with angiotensin antagonist activity.

Also, 2-thenoyl derivatives, as therapeutic agents, exhibit interesting pharmaceutical properties including antimicrobial (Queiroz et al., 2006), anticancer (Thomson et al., 2006), HIV protease inhibitor nelfinavir (Bonini et al., 2004), HIV-PR inhibitors (Bonini et al., 2005), antiinflammatory (Kumar et al., 2004), bacteriostatic and fungistatic activities (Kipnis et al., 1949). Furthermore, they exhibit strong inhibition of NHE-1, cardio-protective efficacy (Lee et al., 2005) and anticancer activity against human renal cells (Nieves-Neira et al., 1999). As well, they are important constituents of many drugs such as methapyrilene, tenidap, tienilic acid and temocillin (Rance and Damani, 1989) (Fig. S1, supplementary information). Consequently, conjugation of pyruvoyl and 2-thenoyl fragments may offer a platform of new antibiotic which synergistic effect of both pharmacophores.

Notably, metal ions not only accelerate the drug action but also enhance the efficacy of the therapeutic agents (Siddiqi et al., 2010). More specifically, metal ions either penetrate into bacterial stain and deactivate their enzymes or generate hydrogen peroxide, thus killing bacteria. Memorable, Cu(II) complexes are known to have a broad spectrum of biological action (Suksrichavalit et al., 2009; Rosu et al., 2010; Kulkarni et al., 2010; Parmar and Kumar, 2009). Currently, the copper compounds used as antifoulants such as metallic copper, cuprous thiocyanate, and cuprous oxide (Comber et al., 2002; Iwao, 2003; Karkhanечи et al., 2013) where the cupric ion (Cu^{2+}) has a major role in antifouling performance in fouling-fighting paints (Yebara et al., 2004). However, the major drawback of copper-based antifouling paint is, the extractable copper concentration in sediment from fish farms using anti-fouling treatment was 2–3 times higher than from those using untreated nets (Nikolaou et al., 2014). Consequently, the use of antifouling paints with inorganic copper additive may be a potential source of copper accumulation in cultured fish. So, researching for new copper alternatives antifouling additives is a topic of increasing interest. To the best of our knowledge, there are a few reports on evaluation of Cu(II) complexes as antifouling agents (Rajalakshmi et al., 2014; Ahmed et al., 2014; Bayer et al., 2011; Hemaida et al., 2008), which give this area exceptional interest to specialist researchers in the field of antifouling.

In the context of our ongoing programs directed toward the development of novel, potent, selective and less toxic therapeutic agents (Wisser and Janiak, 2007; Elshaarawy et al., 2008, 2014; Chamayou et al., 2011; Elshaarawy and Janiak, 2014a,b) and an extension of our previous work on the synthesis thiophen-2-yl derivative (Elshaarawy et al., 2014, 2013; Refat et al., 2014; Elshaarawy and Janiak, 2012; Mahmoud and Janiak, 2009), herein, we now report a concise, practical synthetic route and *in vitro* antimicrobial evaluation as well as anti-biofouling nature of novel thenoylpyruvanthranilic acids (Scheme 1) and their Cu(II) complexes which may be promising antibiotic/anti-biofouling candidates.

2. Experimental

Instrumentation, materials and the preparation details of a series of thenoyl-pyruvoyl-anthranilic acid ligands (**2a–d**) and

enaminones (**3a–e**) can be found in electronic supplementary information.

2.1. Synthesis of the complexes

Generally, 2.0 mmol of the ligand TPAH₂ or TPXAH₂ (cf. Scheme 1) was dissolved in 15 mL of absolute ethanol with a constant stirring/gentle heating. To this solution, 0.399 g (2.0 mmol) of Cu(OAc)₂·H₂O in 10 mL of water was added dropwise with continuous stirring and the pH of the reaction mixture was adjusted to neutral (pH ≈ 6.8) by use of 0.1 M NaOH solution. The reaction mixture was heated under refluxing for 4 h. After cooling slowly, the green precipitates were separated out. The separated compound was filtered, washed thoroughly with absolute ethanol and water, and then dried in a vacuum desiccator with P₂O₅. Unfortunately, many attempts to grow single crystals of these complexes were unsuccessful.

[Cu(TPA)H₂O](**4a**): Yield 83%. FT-IR (ATR, cm⁻¹): 3517 (m, br, $\nu_{(\text{O}-\text{H})}$, H₂O), 3257 (m, br, $\nu_{(\text{N}-\text{H})}$, NHCO), 1675 (s, sh, $\nu_{(\text{C}=\text{O})}$, amide I), 1576 (w, sh, $\nu_{(\text{C}=\text{C}-\text{C}=\text{O})}$), 1516 (m, sh, $\nu_{\text{as}(\text{COO}^-)}$), 1496 (s, sh, $\nu_{(\text{CN})}$ + $\delta_{(\text{N}-\text{H})}$, amide II), 1460 (m, sh, $\nu_{\text{s}(\text{COO}^-)}$), 1351 (m, sh, $\nu_{(\text{CSC})}$, thiophene), 1062 (m, sh, $\nu_{(\text{C}-\text{O})}$, COO⁻), 858, 653, 464; EI-MS *m/z* calcd for C₁₅H₁₁NO₅S: 396.86, found: 396.78. Anal. Calcd. for C₁₅H₁₁CuNO₆S (*M* = 396.86 g/mol): C, 45.40; H, 2.79; N, 3.53; S, 8.08, found: C, 45.44; H, 3.00; N, 3.47; S, 8.23%.

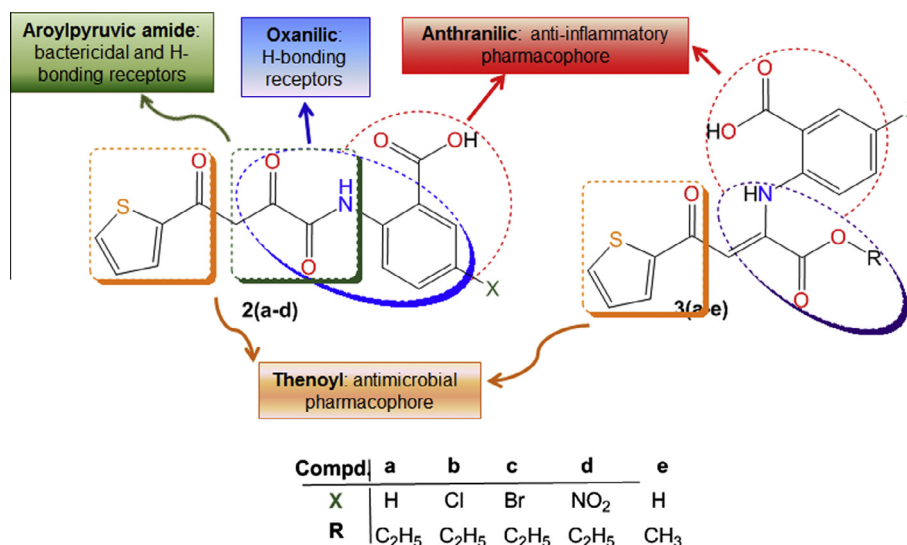
[Cu(TPCA)H₂O](**4b**): Yield 81%. FT-IR (ATR, cm⁻¹): 3444 (m, br, $\nu_{(\text{O}-\text{H})}$, H₂O), 3330 (m, br, $\nu_{(\text{O}-\text{H})}$, H₂O), 3269 (m, br, $\nu_{(\text{N}-\text{H})}$, NHCO), 1592 (s, sh, $\nu_{(\text{C}=\text{O})}$, amide I), 1565 (w, sh, $\nu_{(\text{C}=\text{C}-\text{C}=\text{O})}$), 1495 (m, sh, $\nu_{\text{as}(\text{COO}^-)}$), 1445 (m, sh, $\nu_{\text{s}(\text{COO}^-)}$), 1352 (m, sh, $\nu_{(\text{CSC})}$, thiophene), 1083 (m, sh, $\nu_{(\text{C}-\text{O})}$, COO⁻), 876, 674, 465; EI-MS *m/z* calcd for C₁₅H₁₀ClNO₆SCu: 431.30, found: 431.31; Anal. Calcd. for C₁₅H₁₁CuNO₆S (*M* = 431.30): C, 41.77; H, 2.34; N, 3.25; S, 7.43, found: C, 42.03; H, 2.32; N, 3.23; S, 7.38%.

[Cu(TPBA)H₂O]·H₂O(**4c**): Yield 77%. FT-IR (ATR, cm⁻¹): 3488 (m, br, $\nu_{(\text{O}-\text{H})}$, H₂O), 3330 (m, br, $\nu_{(\text{O}-\text{H})}$, H₂O), 3229 (m, br, $\nu_{(\text{N}-\text{H})}$, NHCO), 1609 (s, sh, $\nu_{(\text{C}=\text{O})}$, amide I), 1571 (w, sh, $\nu_{(\text{C}=\text{C}-\text{C}=\text{O})}$), 1490 (m, sh, $\nu_{\text{as}(\text{COO}^-)}$), 1412 (m, sh, $\nu_{\text{s}(\text{COO}^-)}$), 1350 (m, sh, $\nu_{(\text{CSC})}$, thiophene), 1060 (m, sh, $\nu_{(\text{C}-\text{O})}$, COO⁻), 858, 661, 463; EI-MS *m/z* calcd for C₁₅H₁₂BrNO₇SCu: 431.30, found: 431.31. Anal. Calcd. for C₁₅H₁₂BrCuNO₇S (*M* = 493.77): C, 36.49; H, 2.45; N, 2.84; S, 6.49, found: C, 36.38; H, 2.43; N, 2.39; S, 6.73%.

[Cu(TPNA)(H₂O)₂](**4d**): Yield 68%. FT-IR (ATR, cm⁻¹): 3447 (m, br, $\nu_{(\text{O}-\text{H})}$, H₂O), 3332 (m, br, $\nu_{(\text{O}-\text{H})}$, H₂O), 3176 (m, br, $\nu_{(\text{N}-\text{H})}$, NHCO), 1588 (s, sh, $\nu_{(\text{C}=\text{O})}$, amide I), 1556 (w, sh, $\nu_{(\text{C}=\text{C}-\text{C}=\text{O})}$), 1489 (m, sh, $\nu_{\text{as}(\text{COO}^-)}$), 1425 (m, sh, $\nu_{\text{s}(\text{COO}^-)}$), 1355 (m, sh, $\nu_{(\text{CSC})}$, thiophene), 1081 (m, sh, $\nu_{(\text{C}-\text{O})}$, COO⁻), 846, 665, 459; EI-MS *m/z* calcd for C₁₅H₁₂CuN₂O₉S: 459.87, found: 459.79. Anal. Calcd. for C₁₅H₁₂CuN₂O₉S (*M* = 459.87): C, 39.18; H, 2.63; N, 6.09; S, 6.97, found: C, 39.50; H, 2.71; N, 6.10; S, 6.84%.

2.2. X-ray crystallography

A single crystal with the dimensions of 0.06 × 0.21 × 0.17 mm³ of ethyl 2-thienyl-2-(2-carboxyanilino)-4-oxobutenoate (**3b**) was carefully selected under a polarizing microscope and mounted on a Rigaku *R*-axis Spider diffractometer equipped



Scheme 1 Significant pharmacological sites in thenoyl-pyruvoyl-anthranilic acids (TPXAH₂, **2a-d**) and enaminones (**3a-e**) used in this work.

with sealed tube graphite-monochromatic Mo K α radiation sources ($\lambda = 0.71073 \text{ \AA}$) and image plate (IP) detector. The structure was solved by direct methods (SHELXS-97) (Sheldrick, 2008) and refined using full-matrix least squares on F^2 using the SHELXL-97 program (Sheldrick, 2008); empirical (multi-scan) absorption correction with Abscor (Rigaku) (Higashi, 1995). All non-hydrogen atoms were refined with anisotropic temperature factors. At the final stage of the refinement, H-atoms were positioned geometrically and refined using a riding model (AFIX 43 for aromatic CH, AFIX 13 for aliphatic CH and AFIX 23 for CH₂) with $U_{\text{iso}}(\text{H}) = 1.2U_{\text{eq}}(\text{CH})$. For CH₃ AFIX 33, 133 or 137 was used with $U_{\text{iso}}(\text{H}) = 1.5U_{\text{eq}}(\text{CH}_3)$. The carboxylic H atom has been refined with the riding model AFIX 83 and $U_{\text{iso}}(\text{H}) = 1.5U_{\text{eq}}(\text{O})$. The imine H atom has been refined with the riding model AFIX 43 while the amino nitrogen atoms of 2-aminobenzoic acid have been refined with the riding model AFIX 93. In both cases the (N-H) atoms have been refined with $U_{\text{iso}}(\text{H}) = 1.5U_{\text{eq}}(\text{O})$. The thiophene ring (Th) is disordered about the (O)C-C(Th) bond, depicted in Fig. 1. This thiophene disorder was refined using a PART command.

The asymmetric unit contains half molecule of 2-aminobenzoic acid. The 2-aminobenzoic acid co-crystallite sits on the inversion center as special position. Its unique atoms were refined using PART-n commands because the molecule is disordered on a special position of higher symmetry than the

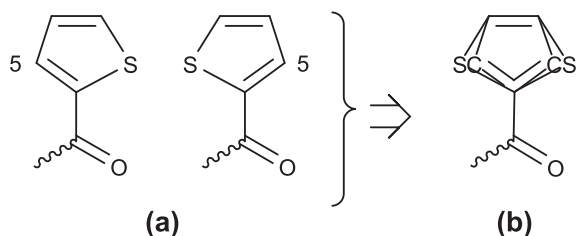


Figure 1 (a) Typical sulfur atom or thiophene ring disorder in the planar ligand and (b) resulting superimposed image in an X-ray structure refinement with approximately half-occupation of the given (5-)C- and S-atom positions.

molecule has itself. Thus, special position constraints are suppressed and bonds to symmetry generated atoms with the same or a different non-zero PART number are excluded. The crystallographic data and refinement parameters are listed in Table 1 (Tables S2, S3, supplementary information). Graphics were drawn with DIAMOND (Brandenburg, 2007–2012).

2.3. Microbiological screening

2.3.1. Antibacterial survey

2.3.1.1. Reagents. Dimethylsulfoxide (DMSO) and Ampicillin antibiotic (C₁₆H₁₉N₃O₄S, 349.41 g mol⁻¹) were obtained from Sigma Chemical Co. (St. Louis, MO, USA).

Table 1 Crystal data and structure refinement for **2b**.

Empirical formula	C ₄₁ H ₃₆ N ₃ O ₁₂ S ₂
Formula weight	826.85 g mol ⁻¹
Temperature (K)	296(2)
Crystal system	Triclinic
Space group	$P - 1 (2)$
a (Å), b (Å), c (Å)	9.5657(3), 10.2949(3), 11.3068(3)
α , β , γ (°)	87.32(0), 77.17(0), 67.33(0)
Volume (Å ³)	1000.84(48)
Z	1
ρ_{calc} (g cm ⁻³)	1.37178
$F(000)$	431
Crystal size	0.06 × 0.21 × 0.17
Theta range for data collection	3.37–27.35°
Index ranges	$-11 \leq h \leq 11$, $-12 \leq k \leq 12$, $-13 \leq l \leq 13$
Reflections collected	16,978
Independent reflections	3865 [$R_{\text{int}} = 0.0251$]
Refinement method	Full-matrix least-squares on F^2
Data/restraints/parameters	3865/0/308
Goodness-of-fit on F^2	1.073
Final R indices [$I > 2\sigma(I)$]	$R_1 = 0.0373$, $wR_2 = 0.0924$
R indices (all data)	$R_1 = 0.0648$, $wR_2 = 0.1141$
Largest diff. peak and hole	0.22 and -0.24 e \AA^{-3}

2.3.1.2. Bacterial cultures. Multi-drug resistant (MDR) strain used in this study from National institute of oceanography and fishery (NIOF), Suez, Egypt. The different strains are penicillin sensitive *Staphylococcus aureus* (PSSA) as representatives for the Gram-positive bacteria and MDREC (multidrug-resistant *Escherichia coli*) (*E. coli*, amoxicillin/clavulanate, trimethoprim/sulfamethoxazole and fluoroquinolone-resistant isolates) as the most important Gram-negative pathogenic bacteria. Stock cultures grown aerobically on nutrient broth (NB) agar slants (Hi-Media) at 37 °C were maintained at 4 °C. Pre-cultures containing 10⁵ CFU/ml, grown aerobically in Mueller Hinton (MH) liquid medium (Hi-Media) at 37 °C for 5 h, were used as inoculum for all experiments.

2.3.1.3. Antimicrobial susceptibility. Antimicrobial susceptibility of the bacterial strains was carried out by agar well diffusion method (Perez and Bazerque, 1990) toward the target compounds as well as standard drugs, Ampicillin. The diameter of the zones of inhibition (ZOI, mm) was measured accurately as indicative of antimicrobial activity.

2.3.1.4. Determination of MIC and MBC. As parameters of the antibacterial efficacy, the minimal inhibitory concentration (MIC) and minimal bactericidal concentration (MBC) of the most potent compounds, Cu(II) complexes (**4a–d**), against infection isolates were determined using the macro-dilution broth susceptibility test. Freshly prepared MH broth was used as diluent in the macro-dilution method. A serial dilution of each target compound was prepared within a desired range (0.25–20.00 mM). One milliliter of the Stock cultures was then inoculated and tubes were incubated at 37 °C for 24 h, control tubes without any addition were assayed simultaneously. MIC was examined visually, by checking the turbidity of the tubes. Furthermore the tubes having lesser concentration than MIC level were inoculated on MHA plate for MBC determination.

2.3.2. Biofilm susceptibility test by Alamar blue method

Whereas, biofilm growth can be used as indicator of biofouling where the sequence of biofilm formation includes (a) adsorption of organic matters and suspended particles on the wetted surface to form a conditioning film; (b) moving of the microbial cells toward the conditioning film and adhesion to the surface; (c) growth and metabolism of the attached microorganisms and biofilm/biofouling development (Nguyen et al., 2012). Consequently, bacterial biofilm formation and antibiotic susceptibility could be used for monitoring surface biofouling.

This test was performed in 96-well non-tissue culture treated microtiter plate. The wells of the titer plate were filled with nutrient broth and inoculated using bacterial culture (0.1 absorbance at 600 nm) so that the final volume comes to 100 mL. Plates were incubated at 37 °C for 24 h without shaking. Complexes were incubated with sterile medium, Cation-Adjusted (Mueller Hinton II. Broth, MHIIB), and DMSO (9:1) external to the plates. After incubation, 50 mL of the suspension was discarded from all the control and test wells and 50 mL of the complex of varying concentration was added (0.25–20 mM). The plates were incubated at 37 °C for 24 h with shaking. After incubation 5 mL of Alamar blue was added to the wells and the plate was incubated at 37 °C for 1 h with gentle shaking. Absorbance at 570 and 600 nm was

recorded using Tecan Infinite M 200 Elisa reader. Positive and negative controls (media alone, media plus AB and cells plus media plus AB) were maintained along with the test (Pettit et al., 2005). The percent reduction of Alamar blue was calculated as follows;

$$\% \text{Reduction of Alamar blue} = \frac{(\epsilon_{\text{ox}})\lambda_2 A \lambda_1 - (\epsilon_{\text{ox}})\lambda_1 A \lambda_2}{(\epsilon_{\text{red}})\lambda_2 A' \lambda_1 - (\epsilon_{\text{red}})\lambda_1 A' \lambda_2} \times 100 \quad (1)$$

here, ϵ_{ox} = molar extinction coefficient of Alamar blue in oxidized form (blue) ϵ_{red} = molar extinction coefficient of Alamar blue in reduced form (pink), A = absorbance of test wells, A' = absorbance of negative control well, λ_1 = 570 nm, λ_2 = 600 nm, ϵ_{ox} = 117,216 at 600 nm and 80,586 at 570 nm, ϵ_{red} = 14,652 at 600 nm and 155,677 at 570 nm.

Notably, although the Alamar blue (AB) reduction method for monitoring biofouling has provided useful information regarding the early formation of biofilms, to date it cannot differentiate between the planktonic growth, biofilm progress and other components deposited on the surface, and cannot provide detailed microbiological/chemical information about the biofilm, therefore their assistance in the development and optimization of efficient anti-fouling strategies is limited.

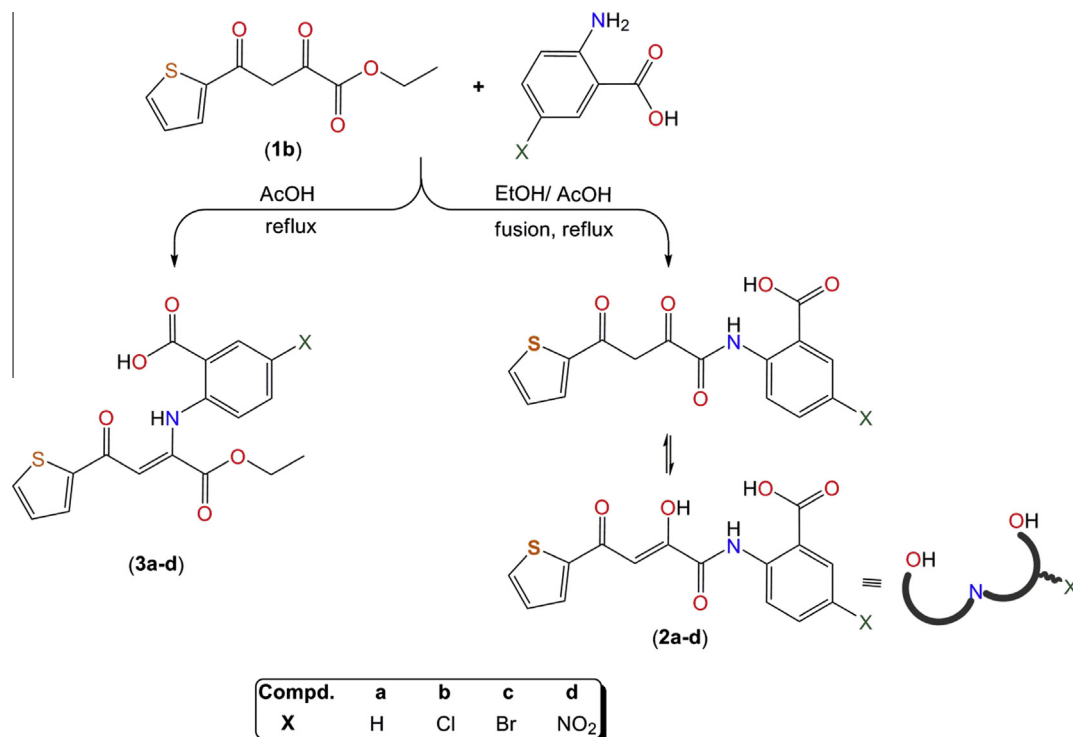
3. Results and discussion

3.1. Synthesis and characterization of ligands

Choosing an appropriate solvent is of crucial importance not only for successful synthesis but also for the effective control of chemoselective reactions. For example, 2-thenoyl-pyruvate **1b** reacted with equimolar amounts of anthranilic acid derivatives in HOAc/EtOH (few drops of HOAc) mixed-solvent system to give thenoyl-pyruvoyl-anthranilide products (α -keto anthranilides). However, if HOAc is used alone, the thienyl-carboxyphenylamino-butenoates (enaminones) were obtained as the main products. Under these optimized chemoselective conditions, a series of thenoyl-pyruvoyl-anthranilic acids (**2a–d**) and enaminones (**3a–e**) were synthesized *via* two component reactions of 2-Thenoyl-pyruvate **1b** and different anthranilic acid derivatives in a mixed-solvent, HOAc/EtOH and single-solvent, HOAc, respectively (see Scheme 2). These compounds have been characterized based on FT-IR, ¹H and ¹³C NMR, elemental analysis and single crystal XRD.

In order to extend the present method to synthesize different enaminones, the aminolysis of thenoyl-pyruvate with different substituted anthranilic acids was explored. Interestingly, the presence of an electron-withdrawing group on the phenyl ring requires longer reaction times with slightly decreased yields.

FTIR spectra of thenoylpyruvanthranilic acids (**2a–d**) revealed the following highlights: (i) Absorptions at the ranges of 3395 ± 25 cm⁻¹ and 1603 ± 27 cm⁻¹ are assignable to the hydroxyl and carbonyl groups stretching vibrations of enolic structural unit (O=C–C=C–OH), respectively. (ii) A broad peak for the N–H stretch of the oxamido group is observed in the range of 3203–3324 cm⁻¹ due to the involvement of amide proton in hydrogen bonding (Krishnapriya et al., 2008). (iii) The broad band centered in the range of 2517–2645 cm⁻¹ is assigned to H-bonded OH stretching frequency of the carboxyl moiety which exhibits additional band, due to carbonyl



Scheme 2 Chemoselective aminolysis of thenoyl-pyruvate with different substituted anthranilic acids.

moiety, around 1695 cm^{-1} . (iv) Three vibrational bands in the range of $1662 \pm 8\text{ cm}^{-1}$, $1602 \pm 28\text{ cm}^{-1}$ and $1513 \pm 5\text{ cm}^{-1}$ were ascribed to the vibrational stretches of the amide I ($\nu_{\text{C=O}}$ of oxamide) (Nakamoto, 1997), amide II ($\delta_{\text{N-H}} + \nu_{\text{C=N}}$) and amide III ($\nu_{\text{C-N}} + \delta_{\text{N-H}}$), respectively (Sahni et al., 1997).

The NMR studies of thenoylpyruvanthranilic acids (**2a-d**) showed that, different substituents on benzoic acid fragment reveal diverse central backbone NMR profiles. For example in TPAH₂ (**2a**), no substituent, the different central backbone is in the enol-oxo-amide tautomeric form and not in the dioxo-amide (keto-oxo-amide) form (Scheme 3). Furthermore, this tautomer must be considered as (Z)-enol- γ -oxo-amide structure as revealed by ¹H-¹H COSY NMR. The prevalence of the (Z)-enol- γ -oxo-amide resonance structure in TPAH₂ ligand could be attributed to intramolecular hydrogen bonding (C=O...H-N) of the enol- γ -oxo-amide arms which led to the formation of a stable six-membered ring system. The ¹H NMR spectrum of TPAH₂ (Fig. S2, supplementary information) exhibits resonances at δ 12.07 ppm for enolic C(8)-OH and at 6.70 ppm for C(7)-vinylic proton typical for enol-oxo-amide form (Belyaev et al., 2002). Further evidence for the prevalence of enolic tautomer is provided by ¹³C NMR spectroscopy, where the absence of NMR signal for the methylene carbon in ¹³C NMR spectrum of TPAH₂ and instead a vinylic carbon signal of the enol-oxo-amide form appears at $\delta \sim 99$ ppm in addition to the downfield signal in the region $\delta \sim 188$ ppm for the enolic carbon.

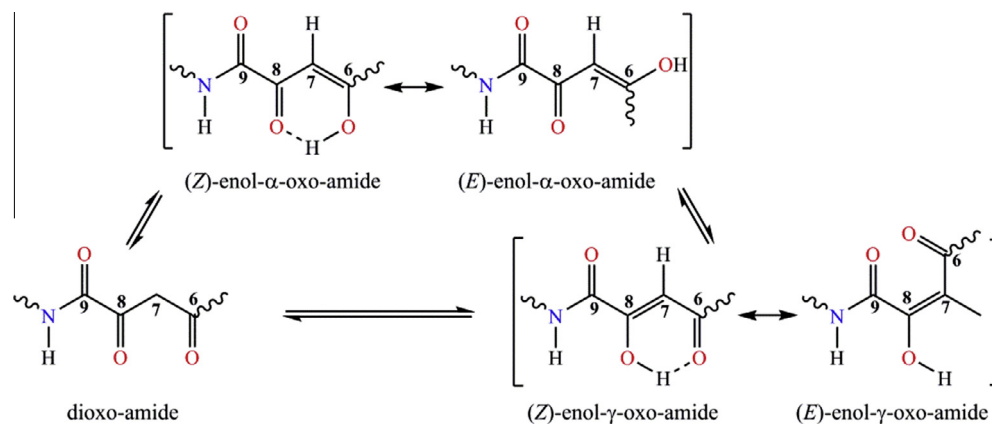
Contrarily, ¹H NMR spectrum of TPBAH₂ (Fig. S3, supplementary information) reveals two singlets at 12.43 ppm for enolic OH and 7.18 ppm for vinylic proton, typical for oxo-enamide tautomeric form of ligand. The singlet at

4.63 ppm, ascribed to geminal CH₂ protons, is also typical for dioxo-amide form of TPBAH₂. Consequently, this ligand must be considered as a resonance hybrid of the (Z)-enol- γ -oxo-amide resonance structure with some contribution of the dioxo-amide resonance structure (Belyaev et al., 2002) (cf. Scheme 3). ¹³C NMR provides additional evidence supporting the coexistence of the oxo-enamide – dioxoamide tautomers. The ¹³C NMR spectrum of TPBAH₂ exhibits a weak resonance at ~ 60 ppm for the methylene carbon and strong signal at ~ 107 ppm for a vinylic carbon of the enol form, additionally, the downfield signal in the region ~ 189 ppm for the enolic carbon and the carbonyl C=O signal of the dione form at ~ 181 ppm.

The ¹H-¹H COSY NMR (Fig. S4, supplementary information) shows the broadened non-coupled singlet at δ 12.3 ppm, which has been assigned as an enolic OH. This indicates that the enolic proton at a considerable distance from thiophene moiety, which suggests that only one tautomeric enol form of the ligands exists in solution under the experimental conditions (enol- γ -oxo-amide).

3.1.1. Crystallographic structure of (**3b**)

X-ray crystallographic data indicates the co-crystallization of ethyl 2-thienyl-2-(2-carboxyanilino)-4-oxobutanoate (ETCAOB) with 2-aminobenzoic acid (anthranilic acid, Anth). ETCAOB and Anth form a 2:1 co-crystal of **3b** in the triclinic space group *P*-1 with *Z* = 1. The asymmetric unit consists of two ETCAOB and one Anth molecules (Fig. S5, supplementary information). H-bonding is dominant interactions in the single crystal structure of **3b**. Major H-bonding interactions (Fig. 2) involved N1-H...O1 (distance of 2.14 Å) and N1-H...O4 (distance of 2.05 Å) in ETCAOB fragment.



Scheme 3 Possible tautomeric forms and intramolecular hydrogen-bonding in backbone of thenoylpyruvanthranilic acids.

X-ray analyses of ETCAOB reveal that it exists in the *Z* form. Noteworthy, the O=C–C=C–N moiety is planar and the bond lengths indicate electron delocalization. The O=C–C=C–N plane is twisted with respect to the benzene and thienyl rings by 34.76(48)° and 21.06(87)°, respectively. Furthermore, the O=C–C=C–N plane and the O=C–O plane make a dihedral angle of 34.96(17)°.

3.2. Synthesis and characterization of Cu(II) complexes

Mononuclear Cu(II) complexes of anthranilides (**2a–d**) have been synthesized from a typical synthetic procedure in which, Cu(OAc)₂·H₂O is reacted with dianionic (*Z*)-enol- γ -oxo-amide core of anthranilide ligands in aqueous ethanol as shown in [Scheme 4](#). These complexes are soluble in DMSO and DMF, slightly soluble in methanol while fairly insoluble in water. The structural and geometrical features of the new complexes were deduced from the elemental and spectral (FTIR, UV–Vis, EIMS) analysis (see Section 2).

FTIR spectra of complexes (**4a–d**) displayed a set of bands at *ca.* 1588–1560 cm^{−1} and 1410–1362 cm^{−1} assignable to the asymmetric $\nu_{as}(\text{COO}^-)$ and symmetric $\nu_s(\text{COO}^-)$ vibrations of coordinated carboxylate group, respectively. The frequency

gaps ($\Delta\nu$) between these bands have an average of ~ 217 cm^{−1} which is consistent with a monodentate coordination mode (η^1) of carboxylate ligation ([Elshaarawy et al., 2014, 2013; Refat et al., 2014; Elshaarawy and Janiak, 2012; Mahmoud and Janiak, 2009](#)). The absence of the characteristic bands at 1730–1690 cm^{−1} for protonated carboxylate and 1603 \pm 27 cm^{−1} for enolate groups indicates the complete deprotonation of the anthranilides ligands which proof that, all ligands coordinate through carboxylate and enolate oxygen atoms. The absence of any significant change in amide I, $\nu\text{C}=\text{O}$, coupled with a negative shift (~ 17 –52 cm^{−1}) of the amide NH band (relative to the free ligand) proves the coordination the amide nitrogen. This further confirmed by the movement of amide II stretch upon coordination toward lower frequency by ~ 22 –28 cm^{−1} (compared to that of free ligand). Moreover, a wide strong band (3500–3300 cm^{−1}) and new band at 856–866 cm^{−1} are due to the O–H stretching and ρOH vibrations, respectively, of the coordinated water molecule. Finally, the $\nu(\text{CSC})$ vibration remains almost unperturbed in all complexes indicating the non-participation of the sulfur atom in coordination ([Elshaarawy and Janiak, 2012](#)). Consequently, our FTIR data revealed that, the anthranilides (**2a–d**) ligands act as ONO tridentate dianionic ligands.

In order to explore the ligand to copper stoichiometric ratios, the UV–Vis titration of TPAH₂ ligand with Cu(II) salt was carried out in aqueous DMSO (9:1 v/v) at 25 °C. Here we take TPAH₂ as representative of these tridentate ligands. As shown in [Fig. 3](#), the 1:1 stoichiometry for the Cu(II)-TPAH₂ complexation was elaborated by the profile of the UV titration curve at 406 nm. These results were in good agreement with those deduced from the elemental analysis and EI-MS studies of complexes **4a**.

The electronic spectra of mononuclear Cu(II) complexes **4a–c** in aqueous DMSO are almost identical. The most characteristic feature of the UV–Vis spectra for these complexes is the broad absorption band in the wavelength range of 369–475 nm which can be assigned to the spin-allowed d-d transition, ${}^2B_{1g} \rightarrow {}^2E_g$. This assignment suggests the square planar geometry for Cu(II) complexes under investigation with [CuO₃N] core ([Lever, 1984; Khana et al., 2009](#)). On the other hand, the electronic spectrum for a five coordinate Cu(II) compound (**4d**) exhibits absorption band near 690 nm due to ${}^2B_{1g} \rightarrow {}^2A_{1g}$ transition supporting an approximate square pyramidal geometry around Cu(II) ion with [CuO₄N] core ([Lever, 1984](#)).

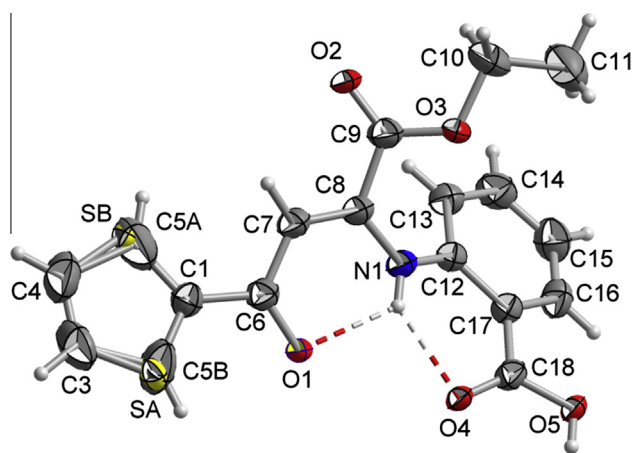
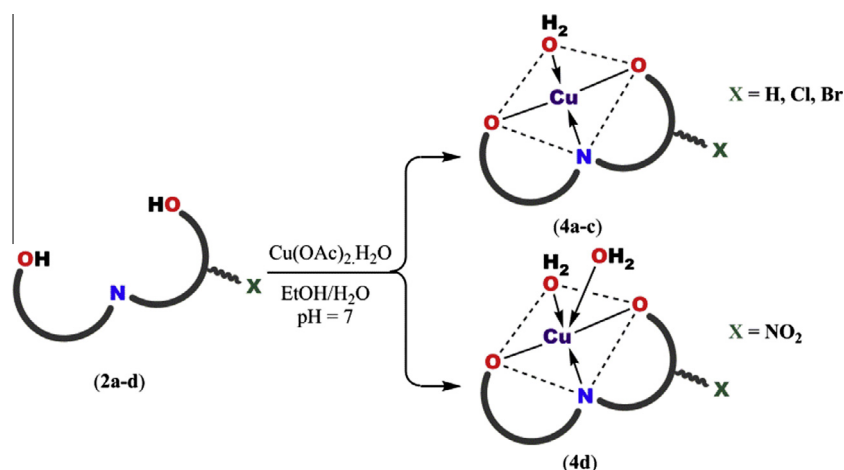


Figure 2 Ellipsoid plot of the *Z*-ETCAOB, showing the atom-labeling scheme and H-bonding interactions.



Scheme 4 Coordination of Cu(II) ion to thenoylpyruvanthranilic acids.

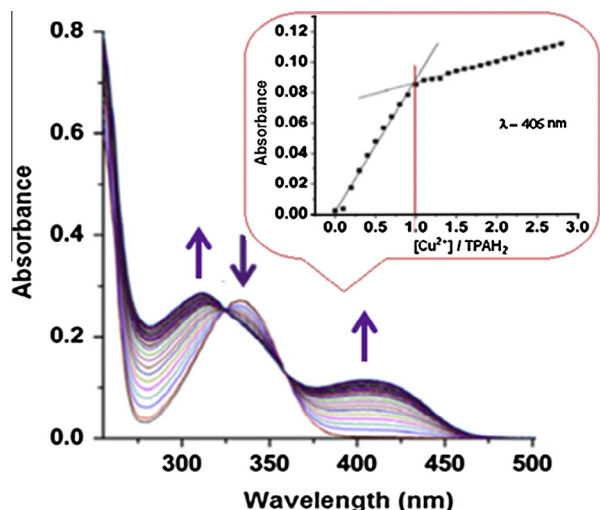
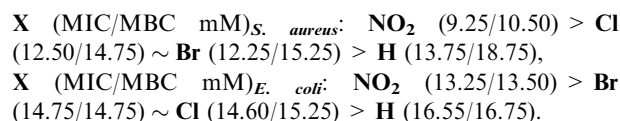


Figure 3 UV-Vis spectra for titration of TPAH₂ (5×10^{-5} M) with Cu²⁺ ion (5×10^{-3} M) in 10% DMSO aqueous solution at r.t.

3.3. Antibacterial activity profile

The target anthranilides (**2a–d**), enaminones (**3a–e**), complexes (**4a–d**) and standards drugs were *in vitro* assessed separately for their capacity to inhibit the growth of two clinically significant pathogenic bacterial strains namely PSSA (*S. aureus*) and MDREC (*E. coli*). Examination of the ZOI (mm) (Table S1, supplementary information) (Fig. 4), MIC and MBC (mM) values (Table 2) for the most potent compounds, (**4a–d**), lead us to highlight the following aspects: (i) All compounds exhibit significant antibacterial efficacy with a higher degree of antistaphylococcal potency than antiescherichia activity and are therefore of interest as potential antistaphylococcal agents. (ii) Noteworthy, the enaminones (**3a–e**), ester derivatives, are more potent than the anthranilides (**2a–d**), amide analogues, while less active than the amide complexes (**4a–d**). (iii) The antibacterial susceptibility was found to depend on the nature

of the substituent attached to the anthranilic moiety. For example, the substituent-dependent antibacterial activity of [Cu(TPBA)(H₂O)_n]·mH₂O (**4a–d**) against *S. aureus* and *E. coli* follows the trend below:



(iv) Cu(II) complex of 2-thenoyl-pyruv-5-nitroanthranilamide, **4d**, exhibits remarkable extra-potent staphylococcal action (MIC/MBC = 9.25/10.50 mM), higher than the standard drug, and thus, can be classified as a new good candidate in the fight against PSSA infections. Further studies are required to explore these complexes as drugs.

In comparison with 2-thenoyl-N-pyruvanthranilic acids (**2a–d**), the observed enhanced antibacterial impact of enaminone esters (**3a–e**) which may be explained by their greater hydrophobicity. This enhanced depolarization facilitates the spontaneous insertion of enaminones into the bacterial membranes, and their conformational flexibility allows better adaptability to the membrane (Bionda et al., 2012).

The enhanced antibacterial activity of the Cu(II) complexes can be explained in terms of Overtone's concept of cell permeability (Dharamaraj et al., 2001) and Tweedy's Chelation theory (Malhotra et al., 1993). Considering these theories, such antibacterial potency of complexes could be assigned to their higher liposolubility effect and enhanced cell permeability owing to diminishing the polarity of the copper ion upon chelation due to the overlap with the ligand orbitals and partial sharing of the positive charge on the copper ion with donor atoms. Further, the delocalization of charge/electrons over the chelate ring enhances the lipophilicity of the complexes. This increased lipophilicity facilitates penetration of these probes into lipid membranes with blocking metal binding sites in the enzymes of microorganisms. These complexes can also disturb the respiration of bacterial cell and thus inhibit protein synthesis that restricts further bacterial growth.

Although the exact mechanism by which antibacterial Cu(II)-thenoylpyruvanthranilates complexes (**4a–d**) exert their

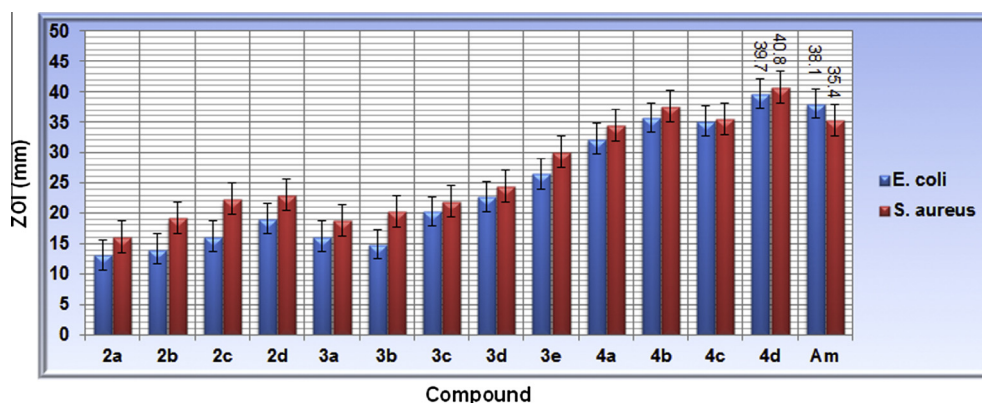


Figure 4 Graph of zone of inhibition (mm) for target compounds against different bacterial species.

Table 2 MIC/MBC (mM) profiles of Cu(II) complexes against different strains.^a

Compound	MIC/MBC (mM)	
	<i>S. aureus</i>	<i>E. coli</i>
4a	13.75/18.75	16.55/16.75
4b	12.50/14.75	14.60/15.25
3c	12.25/15.25	14.75/14.75
4d	9.25/10.50	13.25/13.50
Am.	12.45/NA	15.10/NA

Am. = Ampicillin (Antibacterial drug).

^a *S. aureus* representative for G⁺ Bacteria, *E. coli* as G⁻ Bacteria.

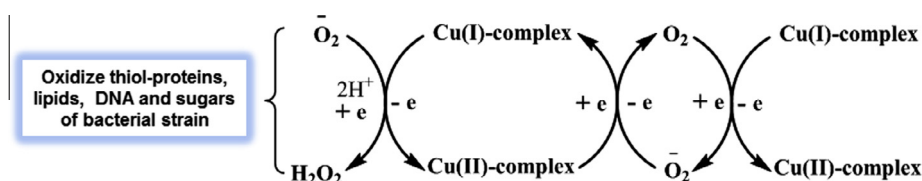
microbiological toxicity has not fully elucidated, their biocidal mode of action may involve various targets in microorganisms: (i) Inhibition of, or interference with cellular envelope biosynthesis inducing envelope damage that can lead to the alteration of cell permeability or disorganized lipoprotein arrangements which ultimately resulted in cell death (Mott et al., 2008). (ii) Hydrogen-bonding interactions of the complex H-receptor sites (such as anilide, carbonyl and carboxylate fragments) with active binding sites of cell constituents, resulting in interference with the normal cell process (Das, 1990). (iii) The redox cycling between Cu(II) and Cu(I) can catalyze the production of highly reactive oxygen species (ROS) such as hydroxyl radicals, thus targeting numerous biochemical pathways within the cell causing oxidation of thiol proteins, DNA damage, lipid peroxidation and the binding-site displacement of Cu-containing metalloprotein (Harrison et al., 2008; Stohs and Bagchi, 1995). Once the Cu(II) complex penetrates the bacterial cell wall, the cellular oxygen oxidizes the protein thiols (R-SH) followed by a one-electron transfer reduction of

copper(II) center to produce Cu(I) complex. Further, oxidation of sulfhydryl group in sulfhydryl-containing proteins (R-S-S-R), such as Cysteine, is another pathway to produce reduced copper complexes. The Cu(II)/Cu(I) complexes system exhibits a relatively high superoxide dismutase (SOD)-like activity, where Cu(I) complex catalyzes the one-electron reduction of normal dioxygen (O₂) to reactive oxygen species (O₂⁻) and peroxide (H₂O₂), while Cu(II) complex may catalyze the dismutation of highly reactive superoxide (O₂⁻) into dioxygen (O₂) (see Scheme 5). The higher reactive oxygen species (ROS) formed during this cycle, superoxide (O₂⁻) and peroxide (H₂O₂), nonspecifically oxidizes lipids, proteins, nucleic acids, and sugars, resulting in staphylococcal effect and *E. coli*-cidal actions. In addition, the reduced Cu(I) complex may inhibit DNA synthesizer ATP production through inhibition of mitochondrial respiration and destruction of cell viability. In conclusion, the quasi-reversible one-electron Cu^{II}/Cu^I redox waves are responsible for the mode of antibacterial action of copper complexes.

3.4. Biofilm susceptibility

The susceptibility of the bacterial biofilm to serial concentrations of the target complexes was carried out by calculating the percentage reduction of Alamar blue for treated *S. aureus* and *E. coli*, spectrophotometrically. Interestingly, from Fig. 5, Cu(II)-TPXA complexes exhibited significant MRSA and MDREC biofilms growth-inhibitory activity at all the examined concentrations and the percentage reduction of Alamar blue varies in a dose-dependent profile.

Our data demonstrate a remarkable biofilm-producing resistance by the action of complex 2a ((Reduction %)_{*S. aureus*-biofilm} = 6.43 at 20 mM; (Reduction %)_{*E. coli*-biofilm} = 10.41 at 20 mM), compared with other complexes. Eventually,



Scheme 5 O₂⁻ dismutation mediated by the SOD [Cu^{II}/Cu^I-complex] redox couple confined in the bacterial species.

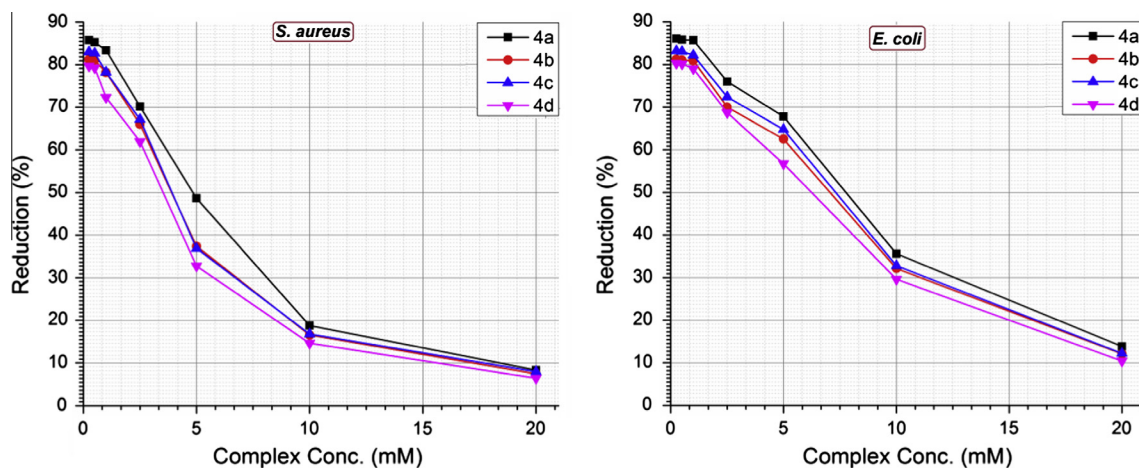


Figure 5 Percent reduction of Alamar blue by *S. aureus* and *E. coli* biofilms treated with different concentrations of complexes (**4a–d**).

refinements of the most active biocidal agent, [Cu(TPNA)(H₂O)₂] (**4d**) may serve as a platform toward discovery of exceptionally active antibiofouling agent to control the formation of biofilm.

4. Conclusion

The present study shows chemoselective aminolysis of 2-thenoyl-pyruvate **1b** with equimolar amounts of anthranilic acid derivatives in either a single solvent, HOAc, to yield enaminones (**3a–e**) or mixed-solvent, HOAc/EtOH (few drops of HOAc), to give α -keto anthranilides (**2a–d**). Mononuclear Cu(II) complexes of anthranilides (**2a–d**) have been synthesized from reaction of (**2a–d**) with Cu(OAc)₂·H₂O. X-ray analyses of ETCAOB, **3b**, reveal the Z form with planar O=C–C=C–N moiety. Antibacterial and antibiofilm susceptibility assay of new copper(II) N-pyruvoyl anthranilate architectures against bacterial marine isolates, *E. Coli* and *S. aureus*, demonstrated that complex **4d** can therefore provide an antibiofilm-forming agent candidate with further chemical refinements. Consequently, future further study for the antifouling performance of **4d** and incorporation of it into the bulk of commercial paint may provide a new generation of antifouling paints.

Acknowledgments

We acknowledge the financial supports of this work by DFG grant Ja466/24-1 (initiation of bilateral cooperation RFME-CJ) and STDF (STDF-STF-Cycle4-6392).

Appendix A. Supplementary material

Contains the supplementary crystallographic data (CIF, TBOAE checkcif) for ligand **3b** (TBOAE). These data can be obtained free of charge via <http://www.ccdc.cam.ac.uk/conts/retrieving.html>, or from the Cambridge Crystallographic Data Centre, 12 Union Road, Cambridge CB2 1EZ, UK; fax: +44 1223 336 033; or e-mail: deposit@ccdc.cam.ac.uk. Supplementary data associated with this article can be found, in the online version, at <http://dx.doi.org/10.1016/j.arabjc.2015.04.010>.

References

- Ahmed, A., Kassim, J., Ghaffi, A.U., Hamdan, H., 2014. *Adv. Mater. Res.*, 204–208.
- Andersen, H.S., Olsen, O.H., Iversen, L.F., Sorensen, A.L.P., Mortensen, S.B., Christensen, M.S., Branner, S., Hansen, T.K., Lau, J.F., Jeppesen, L., Moran, J., Su, J., Bakir, F., Judge, L., Shahbaz, M., Collins, T., Vo, T., Newman, M.J., Ripka, W.C., Moller, N.P.H., 2002. *J. Med. Chem.* 45, 4443–4459.
- Bayer, M., Hellio, C., Marechal, J.-P., Frank, W., Lin, W., Weber, H., Proksch, P., 2011. *Mar. Biotech.* 13 (6), 1148–1158.
- Beaulieu, P.L., Cameron, D.R., Ferland, J.M., Gauthier, J., Ghio, E., Gillard, J., Gorys, V., Poirier, M., Rancourt, J., Wernic, D., Llinas-Brunet, M., Betageri, R., Cardozo, M., Hickey, E.R., Ingraham, R., Jakes, S., Kabcenell, A., Kirrane, T., Lukas, S., Patel, U., Proudfoot, J., Sharma, R., Tong, L., Moss, N., 1999. *J. Med. Chem.* 42, 1757–1766.
- Belyaev, E.S., Berezina, V.O., Koźminykh, R.R., Makhmudov, S., Odegova, T.F., 2002. *Pharm. Chem. J.* 36 (12), 9–11.
- Bionda, N., Stawikowski, M., Stawikowska, R., Cudic, M., Lopez-Vallejo, F., Treitl, D., Medina-Franco, J., Cudic, P., 2012. *ChemMedChem* 7, 871–882.
- Bonini, C., Chiummiento, L., De Bonis, M., Funicello, M., Lupattelli, P., 2004. *Tetrahedron Lett.* 45, 2797–2800.
- Bonini, C., Chiummiento, L., De Bonis, M., Funicello, M., Lupattelli, P., Suanno, G., Bertib, F., Campaner, P., 2005. *Tetrahedron* 61, 6580–6589.
- Brandenburg, K., 2007–2012. *Diamond (Version 3.2h)*, Crystal and Molecular Structure Visualization, Crystal Impact. K. Brandenburg & H. Putz Gbr, Bonn, Germany.
- Chamayou, A.-C., Neelakantan, M.A., Thalamuthu, S., Janiak, C., 2011. *Inorg. Chim. Acta* 365, 447–450.
- Comber, S.D.W., Franklin, G., Gardner, M.J., 2002. *Sci. Total Environ.* 286, 61–71.
- Das, A.K. (Ed.), 1990. *Medicinal Aspects of Bioinorganic Chemistry*, Chapter 3. CBS, Shahdara, Delhi.
- Dharamaraj, N., Viswanathamurthi, P., Natarajan, K., 2001. *Transition Met. Chem.* 26, 105–109.
- Elshaarawy, R.F.M., Janiak, C., 2012. *Z. Naturforsch.* 66b, 1202–1208.
- Elshaarawy, R.F.M., Janiak, C., 2014a. *Tetrahedron* 70, 8023–8032.
- Elshaarawy, R.F.M., Janiak, C., 2014b. *Eur. J. Med. Chem.* 75, 31–42.
- Elshaarawy, R.F.M., Ibrahim, H.K., Eltamany, E., Mohy-Eldeen, I., 2008. *Maced. J. Chem. Chem. Eng.* 27 (1), 65–79.
- Elshaarawy, R.F.M., Lan, Y., Janiak, C., 2013. *Inorg. Chim. Acta* 401, 85–94.

- Elshaarawy, R.F.M., Kheiralla, Z.H., Rushdy, A.A., Janiak, C., 2014. *Inorg. Chim. Acta* 421, 110–122.
- Hargrave, H.D., Hess, F.K., Oliver, J.T., 1983. *J. Med. Chem.* 26, 1158–1163.
- Harrison, J.J., Turner, R.J., Joo, D.A., Stan, M.A., Chan, C.S., Allan, N.D., Vrionis, H.A., Olson, M.E., Ceri, H., 2008. *Antimicrob. Agents Chemother.* 52, 2870–2881.
- Hemaida, H.A.E., El-Dissouky, A., Sadek, S.M.M., 2008. *Pigment Resin Tech.* 37 (4), 243–249.
- Higashi, T., 1995. ABSCOR. Rigaku Corporation, Tokyo, Japan.
- Iversen, L.F., Andersen, H.S., Moller, K.B., Olsen, O.H., Peters, G.H., Branner, S., Mortensen, S.B., Hansen, T.K., Lau, J., Ge, Y., Holsworth, D.D., Newman, M.J., Moller, N.P.H., 2001. *Biochemistry* 40, 14812–14820.
- Iversen, L.F., Moller, K.B., Pedersen, A.K., Peters, G.H., Petersen, A.S., Andersen, H.S., Branner, S., Mortensen, S.B., Moller, N.P.H., 2002. *J. Biol. Chem.* 277, 19982–19990.
- Iwao, O., 2003. *Chem. Rev.* 103, 3431–3448.
- Karkhanechi, H., Takagi, R., Ohmukai, Y., Matsuyama, H., 2013. *Desalination* 325, 40–47.
- Khana, T.A., Naseem, S., Khan, S.N., Khan, A.U., Shakir, M., 2009. *Spectrochim. Acta A73*, 622–629.
- Kipnis, F., Soloway, H., Ornfelt, J., 1949. *J. Am. Chem. Soc.* 71, 10–11.
- Klaubert, D.H., Sellstedt, J.H., Guinosso, C.J., Capetola, R.J., Bell, S.C., 1981. *J. Med. Chem.* 24, 742–748.
- Koźminykh, V.O., Igidov, N.M., Lienko, V.I., 1992. *Khim.-Farm. Zh.* 26, 28–31.
- Koźminykh, E.N., Belyaev, A.O., Berezina, E.S., 2002. *Khim.-Farm. Zh.* 36 (12), 9–11.
- Krishnapriya, K.R., Saravanakumar, D., Arunkumar, P., Kandaswamy, M., 2008. *Spectrochim. Acta A69*, 1077–1081.
- Kulkarni, N.V., Hegde, G.S., Kurdekar, G.S., Budagumpi, S., Sathisha, M.P., Revankar, V.K., 2010. *Spectrosc. Lett.* 43, 235–246.
- Kumar, P.R., Raju, S., Goud, P.S., Sailaja, M., Sarma, M.R., Reddy, G.O., Kumar, M.P., Lee, S., Lee, H., Lee, Y.K., Yoo, S., Lee, K., Cho, N.S., 2004. *Bioorg. Med. Chem. Lett.* 15, 2998–3001.
- Lever, A.B.P., 1984. *Inorganic Electronic Spectroscopy*, second ed. Elsevier, Amsterdam.
- Mahmoud, R.F., Janiak, C., 2009. *Acta Cryst. E65*, m909–m910.
- Malhotra, R., Kumar, S., Dhindsa, K.S., 1993. *Indian J. Chem.* 32A, 457–459.
- Matsoukas, J., Cordopatis, P., Belte, U., Goghari, M.H., Ganter, R.C., Franklin, K.J., Moore, G.J., 1988. *J. Med. Chem.* 31, 1418–1421.
- Milyutin, A.V., Amirova, L.R., Krylova, I.V., 1997. *Khim.-Farm. Zh.* 31 (1), 32–35.
- Mott, J.E., Shaw, B.A., Smith, J.F., Bonin, P.D., Romero, D.L., Marotti, K.R., Miller, A.A., 2008. *J. Antimicrob. Chemother.* 62, 720–729.
- Nakamoto, K., 1997. *Infrared and Raman Spectra of Inorganic and Coordination Compounds*, fifth ed. John Wiley, New York, Part B.
- Nguyen, T., Roddick, F.A., Fan, L., 2012. *Membranes* 2, 804–840.
- Nieves-Neira, W., Rivera, M., Kohlhagen, G., Hursey, M.L., Pourquier, P., Sausville, E.A., Sausville, Y.P., 1999. *Mol. Pharm.* 56, 478–484.
- Nikolaou, M., Neofitou, N., Skordas, K., Castritsi-Catharios, I., Tziantziou, L., 2014. *Aquacult. Environ. Interact.* 5, 163–171.
- Parmar, S., Kumar, Y., 2009. *Chem. Pharm. Bull.* 57, 603–606.
- Perez, C., Bazerque, P., 1990. *Acta Biol. Med. Exp.* 15, 113–115.
- Pettit, R.K., Weber, C.A., Kean, M.J., Hoffman, H., Pettit, G.R., Tan, R., Franks, K.S., Horton, M.L., 2005. *Antimicrob. Agents Chemother.* 49, 2612–2617.
- Queiroz, M.R.P., Ferreira, I.C.F., Gaetano, Y.D., Kirsch, G., Calhelha, R.C., Estevinho, L.M., 2006. *Bioorg. Med. Chem.* 14, 6827–6831.
- Rajalakshmi, S., Fathima, A., Raghava, J., Nair, U.B., 2014. *RSC Adv.* 4, 32004–32012.
- Rance, D.J., Damani, L.A., 1989. *Sulfur-Containing Drugs and Related Organic Compounds* Chichester. Ellis Horwood, West Sussex, England, 217.
- Refat, M.S., El-Deen, I.M., Elshaarawy, R.F., 2014. *Russ. J. Gen. Chem.* 84 (3), 593–601.
- Rosu, T., Pahontu, E., Pasculescu, S., Georgescu, R., Stanica, N., Cura, A., Popescu, A., Leabu, M., 2010. *Eur. J. Med. Chem.* 45, 1627–1634.
- Sahni, S.K., Gupta, S.P., Sangal, S., Rana, V.B., 1977. *J. Indian Chem. Soc.* 54, 200–208.
- Sellstedt, J.H., Guinosso, C.J., Begany, A.J., Bell, S.C., Rosenthale, M., 1975. *J. Med. Chem.* 18, 926–933.
- Sheldrick, G.M., 2008. *Acta Crystallogr. A* 64, 112–122.
- Siddiqi, Z.A., Khalid, M., Kumar, S., Shahid, M., Noor, S., 2010. *Eur. J. Med. Chem.* 45 (1), 264–269.
- Stoys, S.J., Bagchi, D., 1995. *Free Radical Biol. Med.* 18, 321–336.
- Suksrichavalit, T., Prachayasittikul, S., Nantasenammat, C., Ayudhya, C.I.N., Prachayasittikul, V., 2009. *Eur. J. Chem.* 44, 3259–3265.
- Thomson, P., Naylor, M.A., Everett, S.A., Stratford, M.R.L., Lewis, G., Hill, S., Patel, K.B., Wardman, P., Davis, P., 2006. *Mol. Cancer Therapeut.* 5, 2886–2894.
- Wisser, B., Janiak, C., 2007. *Z. Anorg. Allg. Chem.* 633, 1796–1800.
- Wright, J.B., Johnson, H.G., 1977. *J. Med. Chem.* 20, 166–169.
- Yanborisov, T.N., Shurov, S.N., Andreichikov, Yu.S., 1989. *Khim.-Farm. Zh.* 23 (12), 1470–1473.
- Yebra, D.M., Kiil, S., Dam, J.K., 2004. *Prog. Org. Coat.* 50, 75–104.